

ELECTRON BEAM WELDING OF DISSIMILAR METALS AND ALLOYS

**Darina Kaisheva^{1,2}, Georgi Kotlarski¹, Borislav Stoyanov³, Vladimir Dunchev³,
Maria Ormanova¹, Stefan Valkov^{1,3}**

¹*Academician Emil Djakov Institute of Electronics, Bulgarian Academy of Sciences, 72
Tzarigradsko Chausse Blvd, 1784 Sofia, Bulgaria*

²*South-West University „Neofit Rilski“, 66 Ivan Michailov Str., 2700 Blagoevgrad, Bulgaria*

³*Technical University of Gabrovo, 4 H. Dimitar Str., 5300 Gabrovo, Bulgaria*

Abstract

In this work, we present results on the investigation of the structure and mechanical properties of electron beam welded specimens of copper and stainless steel, copper and aluminum alloy, and titanium and titanium Ti6Al4V alloy. The structure of the fusion zone of all samples was studied by scanning electron microscopy (SEM) and energy-dispersive X-ray spectroscopy (EDX) analysis, and its phase composition – by X-ray diffraction (XRD) analysis. The mechanical properties were investigated by tensile tests and microhardness measurements. The results for the mechanical properties were discussed concerning the applied technological conditions and the structure of the welded joints.

Keywords: electron beam welding, dissimilar materials, stainless steel, copper, aluminum alloy, titanium, titanium alloy.

INTRODUCTION

Different technologies are used to join dissimilar materials. An overview article [1] describes the most commonly used techniques and technologies for joining dissimilar materials: mechanical joining processes, chemical joining processes, thermal fusion joining processes, including electric arc welding, laser beam welding and electron beam welding, and hybrid joining processes.

The electron beam welding (EBW) method has been intensively used in modern industrial production, mainly in the automotive industry, aircraft construction, shipbuilding, etc. due to its significant advantages compared to other welding methods. Among the main advantages of electron beam welding over other methods are: high power density, high welding speed, which allows the formation of very narrow and deep welds, the presence of a protective vacuum environment, etc. In EBW, the kinetic energy of a beam of accelerated electrons with a very high energy density (over 10^6 W/cm²) is converted into heat, accompanied by sharp

heating, melting and vaporization of the processed metals. A vapor-gas channel called a “keyhole” is formed, consisting of superheated vapor in the medium surrounded by liquid metal [2, 3]. Complex physical and physical-chemical processes take place in the molten pool under the action of various forces [4]. The heating and cooling processes of the molten metal in the region of the weld seam, as well as the metal in the heat-affected zone, is carried out at very high speeds. As a result, phase transformations occur, which, together with large temperature gradients, lead to the appearance of residual stresses and deformations. Due to the different materials that fuse together, in many cases intermetallic compounds are formed in the weld zone, which are often brittle and make the joint unsustainable. In [5], an overview of the weldabilities of dissimilar materials using the EBW method was made.

There are a number of studies that describe the welding of materials with different thermophysical properties by the electron

beam welding method [6-11]. The main goal of the research is based on the need to obtain composite structures in the weld seam by combining two different materials, preserving the advantages of the properties possessed by each material separately. Good weld quality is largely determined by the crystallographic structure and the presence of intermetallic phases.

The aim of the present work is to characterize the structure and mechanical properties of specific pairs of dissimilar materials concerning the applied technological conditions during the EBW. We have focused our attention on light metals (copper, titanium, aluminum) due to their importance for a variety of practical applications [12-18]. In this work, we present results on the investigation of the structure and mechanical properties of electron beam welded specimens of copper and stainless steel, copper and aluminum alloy, and titanium and Ti6Al4V alloy.

METHODS AND MATERIALS

The subjects of our investigation were the following three types of electron beam welded samples: copper and 304L stainless steel; copper and Al 6082 T6 aluminum alloy; titanium and Ti6Al4V titanium alloy (Ti64). The chemical composition of listed alloys is shown in Table 1.

Table 1. The chemical composition of studied alloys.

304L		Al 6082 T6		Ti6Al4V	
El.	wt, %	El.	wt, %	El.	wt, %
C	0.03	Si	1.3	Al	5.5
Mn	1.52	Mg	1.0	V	4.5
Si	0.10	Mn	0.8	Fe	0.3
P	0.03	Fe	0.2	Ti	Bal.
S	0.03	Cr	0.1		
Cr	17.70	Al	Bal.		
Ni	8.30				
N	0.10				
Fe	Bal.				

Electron beam welding was carried out on the Evobeam Cube 400 welding unit manufactured by Evobeam. Plates with dimensions of 100x50x8 mm of two different materials were joined via EBW. The technological parameters of EBW were different for

different welded couples and are shown in Table 2.

Table 2. Technological conditions of EBW.

Sample	Cu / 304L	Cu / Al6082T6	Ti / Ti6Al4V
Accelerating voltage U_a , kV	60	60	60
Beam current I , mA	50	50	35
Welding speed v , mm/s	5	15	10
Offset	-	0.4 mm towards Al 6082 T6	-
Beam oscillation	-	circle $r_{osc.}=0.1$ mm	-

X-ray diffractometer (XRD) “Bruker D8 Advance” was used for phase analysis. The method was “Coupled Two Theta”, using Co $K\alpha$ radiation with wavelength 1.78897 Å and line focus orientation. The X-ray generator current was 40 mA and the used voltage was 35 kV. The step size of the test was 0.05° and the time for the step was 0.25 s.

ZwickRoell Vibrophore 100 combined static and dynamic testing machine was used for mechanical characteristics determination. Microhardness measurement was performed using the Vickers method. Determination of microhardness for all experimental points was performed with a force load of 0.49 N using a semi-automatic microhardness tester ZWICK/Indentec - ZHV μ -S. The line along which the microhardness was measured is located at middle depth of the weld seam.

RESULTS AND DISCUSSION

Electron beam welding of Cu and 304L stainless steel

The X-ray diffraction patterns of the welded copper-stainless steel specimen, pure copper, and 304L are shown in Fig. 1. The presence of two phases is visible – a solid solution of copper and γ -iron (with a face centered cubic crystal lattice fcc) and α -iron (with a body centered cubic crystal lattice bcc). The appearance of the metastable phase of α -iron is associated with the large temperature gradients that occur in the electron beam welding procedure.

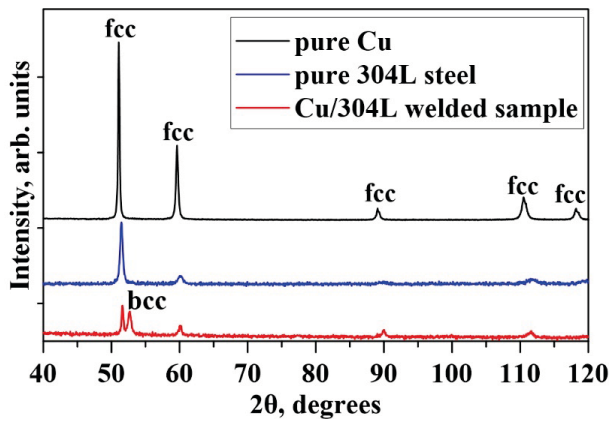


Fig. 1. X-ray patterns of the welded copper-stainless steel specimen, pure copper and pure 304L steel.

The observed structure of the SEM image (Fig. 2) confirms the presence of the two phases mentioned above in the fusion zone.

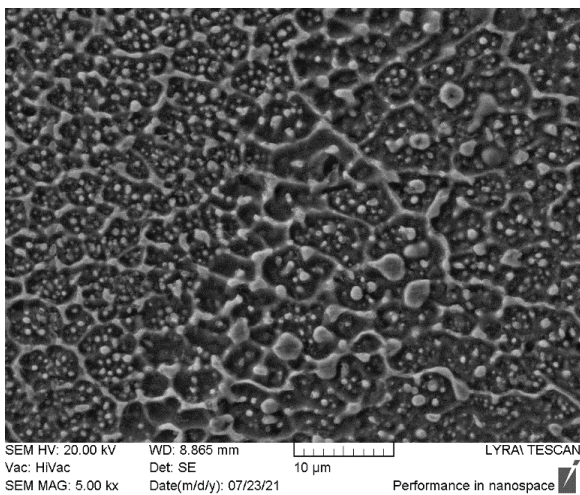


Fig. 2. SEM image of the fusion zone of the welded Cu/304L sample.

Table 3 shows the measured values of the mechanical properties of the initial materials and the welded joint. The measured values for the tensile strength of the weld as well as the elongation are within close range of those of pure copper.

Table 3. Tensile test results of Cu/304L weld.

Material	Yield strength $R_{p0.2}$, MPa	Tensile strength R_m , MPa	Total extension A_t , %
Pure Cu	267	275	16.8
Pure 304L	298	608	35.8
Cu/304L	93	218	14.6

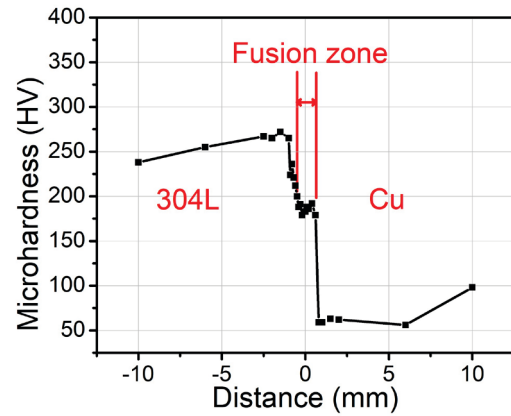


Fig. 3. Distributions of the microhardnesses along the weld cross-section in the middle of the depth of the Cu/304L weld.

The microhardness distribution in the middle of the weld along the cross-section is shown in Fig. 3. In the fusion zone, intermediate hardness values to those of pure copper and pure stainless steel are observed.

Electron beam welding of Cu and Al6082T6 alloy

Electron beam offset and electron beam oscillation were applied to the making of a copper/aluminum alloy sample. The beam offset was towards the aluminum alloy side. The electron beam oscillation was a circular.

The X-ray diffraction patterns of the welded copper-aluminum alloy specimen, pure copper, and Al6082T6 are shown in Fig. 4. The main phase observed in the fusion zone is $CuAl_2$ with a body-centered tetragonal structure. In addition, aluminum and copper peaks having a face-centered cubic structure are also observed.

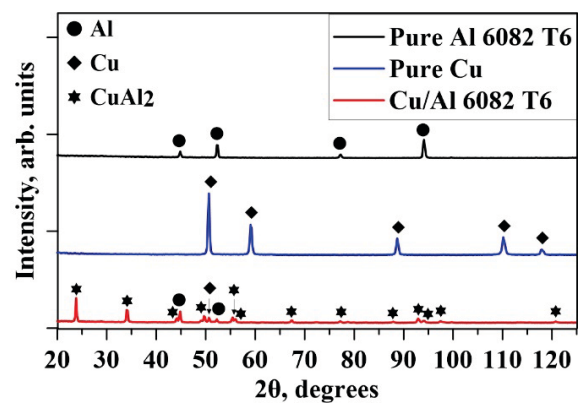


Fig. 4. X-ray patterns of the welded copper-aluminum alloy specimen, pure copper, and pure Al 6082 T6.

The fusion zone of the specimen contains three phases – an aluminum matrix, an ordered solid solution of copper and aluminum in the form of CuAl_2 , and pure copper in the region towards the copper plate, as can also be seen from the SEM image shown in Figure 5.

The studied sample did not show satisfactory strength in the tensile tests.

In Fig. 6, the microhardness distribution in the cross-section of the welded Cu/Al 6082 T6 sample is shown. At both edges of the fusion zone there is a significant increase in hardness compared to the initial materials. The reason for this is the above-mentioned intermetallic phase.

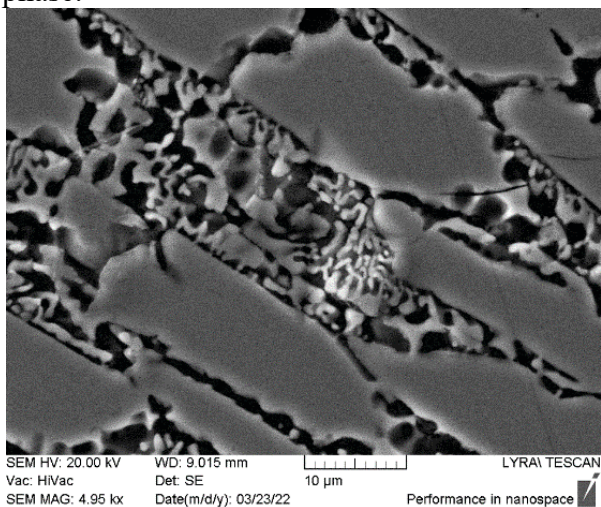


Fig. 5. SEM image of the fusion zone of the welded Cu/Al 6082 T6 sample.

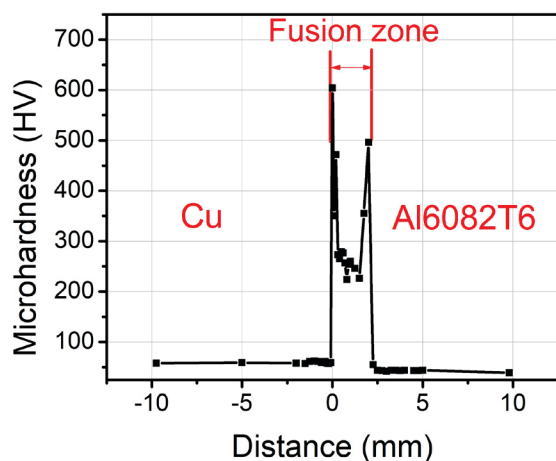


Fig. 6. Distributions of the microhardnesses along the weld cross-section in the middle of the depth of the Cu/Al6082T6 weld.

Electron beam welding of Ti and Ti6Al4V alloy

The two initial materials have a similar chemical composition, but quite different thermophysical characteristics. The phase composition of the welded joint, as well as of the pure Ti and Ti6Al4V samples were studied by XRD experiments.

Considering the pure Ti plate, its phase composition is in the form of a single-phase of α -titanium. In contrast, the structure of the titanium alloys is in the form of a double-phase of $\alpha+\beta$. It is well known that β is the high-temperature modification of Ti and is stable above 1153 K. However, the appearance of this phase can be not only due to high-temperature reasons. It could be attributed also due to the existence of β stabilizing elements, such as Ta, Nb, V, etc. As mentioned previously, 4 at. % V exists within the titanium alloy, which is the reason for the appearance of the beta phase at room temperature. The structure of the welded joint is in the form of a single-phase α' martensite, formed due to the very large cooling rate during the welding procedure.

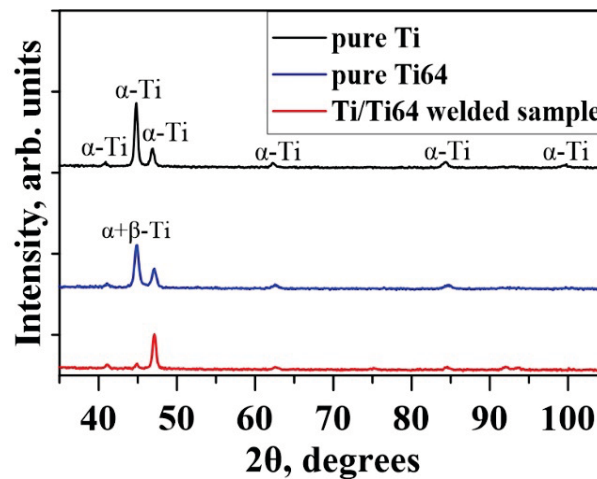


Fig. 7. X-ray patterns of the welded titanium-titanium alloy specimen, pure titanium, and pure Ti64.

In the SEM image of the fusion zone (Fig.8) it is seen that there is no presence of the β -phase of Ti. The formed martensitic structure in the weld seam is clearly visible.

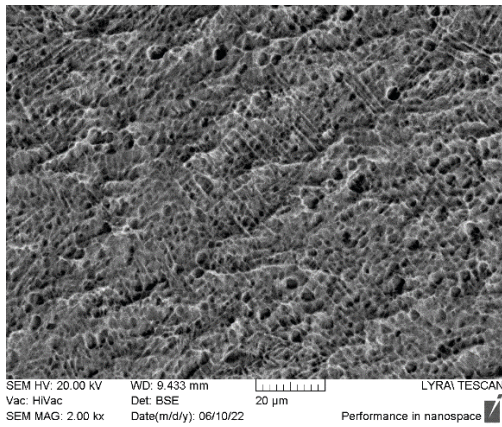


Fig. 8. SEM image of the fusion zone of the welded Ti/Ti6Al4V sample.

The measured values of yield strength, tensile strength and relative elongation of the initial materials and the welded joint are shown in Table 4. The achieved tensile strength of the weld is practically equivalent to that of pure titanium.

Table 4. Tensile test results of Ti/Ti6Al4V weld.

Material	Yield strength $R_{p0.2}$, MPa	Tensile strength R_m , MPa	Total extension A_t , %
Pure Ti	372	511	22.1
Pure Ti6Al4V	1031	1064	10.6
Ti/Ti6Al4V	125	510	17.4

The microhardness distribution along the cross-section of the weld is shown in Fig. 9. Increased hardness is observed in the fusion zone, which is due to the resulting martensitic structure. A rise in the hardness is also seen in the surrounding heat affected zones of both materials, again due to the phase transitions resulting from the high temperature gradients at EBW.

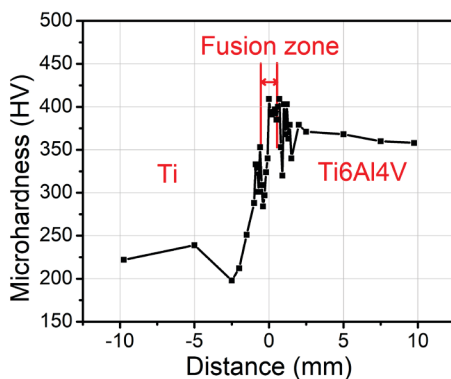


Fig. 9. Distributions of the microhardnesses along the weld cross-section in the middle of the depth of the Ti/Ti6Al4V weld.

CONCLUSION

In this paper, we demonstrated the possibilities for the fabrication of welded joints between dissimilar metals and alloys using electron beam technologies. Precisely selected technological conditions during the welding process led to obtaining strong and unbreakable welds. On the other hand, it contributes to the improvement of the mechanical characteristics (hardness, yield and, tensile strength) of the joints. These properties are very important for the implementation of dissimilar joints in various branches of modern industry.

ACKNOWLEDGEMENTS

This work was supported by Bulgarian National Scientific Found under Grant No KP06-N47/6.

REFERENCE

- [1] Martinsen K, Hu SJ, Carlson BE, Joining of dissimilar materials. *CIRP Annals* 64(2) (2015) 679-699.
- [2] Шиллер З, Гайциг У, Панцер З, *Электронно-лучевая технология*, Москва, изд. Энергия (1980).
- [3] Mihailov V, Karhin V, Petrov P, *Fundamentals of welding* (In English), Polytechnic University Publishing, St. Petersburg (2016).
- [4] Weglowski M, Błacha S, Phillips A, Electron beam welding-Techniques and trends-Review. *Vacuum* 130 (2016) 72-92.
- [5] Sun Z, Karppi R, The application of electron beam welding for the joining of dissimilar metals: an overview. *Journal of Materials Processing Technology* 59(3) (1996) 257-267.
- [6] Guo S, Zhou Q, Peng Y, Xu XF, Diao CL, Kong J, Luo TY, Wang KH, Zhu J, Study on strengthening mechanism of Ti/Cu electron beam welding. *Materials & Design* 121 (2017) 51-60.
- [7] Chen G, Yin Q, Guo C, Zhang B, Feng J, Beam deflection effects on the microstructure and defect creation on electron beam welding of molybdenum to Kovar. *Journal of Materials Processing Technology* 267 (2019) 280-288.
- [8] Dinda SK, Kar J, Roy GG, Kockelmann W, Srirangam P, Texture mapping in electron beam welded dissimilar copper-stainless steel joints by neutron diffraction. *Vacuum* 181 (2020) 109668.

- [9] Roy, C, Pavanan V, Vishnu G, Hari PR, Arivarasu M, Manikandan M, Ramkumar D, Arivazhagan N, Characterization of metallurgical and mechanical properties of commercially pure copper and AISI 304 dissimilar weldments. *Procedia Materials Science* 5 (2014) 2503 – 2512.
- [10] Yeganeh VE, Li P, Effect of beam offset on microstructure and mechanical properties of dissimilar electron beam welded high temperature titanium alloys. *Materials Design*, 124 (2017) 78–86.
- [11] Wang SQ, Liu JH, Chen DL, Tensile and fatigue properties of electron beam welded dissimilar joints between Ti-6Al-4V and BT9 titanium alloys. *Materials Science & Engineering A*, 584 (2013) 47–56.
- [12] Kovalev SV, Portnykh AI, Aslamova VY, Research of Ti-6Al-4V titanium alloy welded joints made by electron beam welding, designed for operation in cryogenic conditions. *IOP Conference Series: Materials Science and Engineering* 971 (2020) 022005.
- [13] Fujii H, Takahashi K, Yamashita Y, Application of Titanium and Its Alloys for Automobile Parts. *Nippon Steel Technical Report* 88 (2003) 70–75.
- [14] Kaur S, Ghadirinejad K, Oskouei RH, An Overview on the Tribological Performance of Titanium Alloys with Surface Modifications for Biomedical Applications. *Lubricants* 7(8) (2019) 65–80.
- [15] Williams JC, Boyer RR, Opportunities and Issues in the Application of Titanium Alloys for Aerospace Components. *Metals* 10(6) (2020) 705.
- [16] Schauerte O, Titanium in automotive production. *Advanced Engineering Materials* 5(6) (2003) 411–418.
- [17] Lusch C, Börsch M, Heidt C, Maggini N, Sas J, Weiss KP, Grohmann S, Qualification of Electron-Beam Welded Joints between Copper and Stainless Steel for Cryogenic Application. *IOP Conference Series: Materials Science and Engineering* 102 (2015) 012017.
- [18] Poo-arporn Y, Duangnil S, Bamrungkoh D, Klangkaew P, Huasranoi C, Pruekthaisong P, Boonsuya S, Chairapa J, Ruangvittayanon A, Saisombat C, Gas tungsten arc welding of copper to stainless steel for ultra-high vacuum applications. *Journal of Materials Processing Technology* 277 (2020) 116490.